Visualization of Flow Characteristics in a 2-D Bubble Column and Three-Phase Fluidized Bed

J.-W. Tzeng, R. C. Chen, and L.-S. Fan
Dept. of Chemical Engineering, The Ohio State University, Columbus, OH 43210

Macroscopic flow structures of gas-liquid and gas-liquid-solid fluidization systems are studied through flow visualization using a two-dimensional column under various operating conditions. The gas distributor in the column comprises multiple injectors which are individually regulated to generate desired gas flow rates, bubble injection frequencies, and bubble sizes. Colored bed particles and neutrally buoyant particles as solid and liquid tracers, respectively, are used for flow visualization through video photography. In a gas-liquid system operated under liquid-batch conditions, bubble streams injected near both sidewalls are observed to migrate toward bed vertical axis, and vortices appear along the sidewalls when gas velocity exceeds 4–6 mm/s. A considerable amount of liquid descends along the sidewalls in a vortical flow pattern. The gross circulation pattern occurring at high gas velocities is associated closely with induced liquid or liquid-solid flows resulting from rising bubbles and bubble wakes. When the gross circulation occurs, four flow regions can be distinguished. The formation of and mechanism for gross circulations can be interpreted in part based on two simplified flow conditions involving single bubbles rising in a stationary liquid and single chains of bubbles injected in a batch liquid. The effects of particle size, inlet liquid velocity and gas flow distribution on the macroscopic flow structure are also examined.

Introduction

Bubble or slurry bubble column systems can be operated under bubbly, churn-turbulent or slugging regimes based on bubble dynamics (Fan, 1989). The gross circulation flow pattern has been observed for these systems under both bubbly and churn-turbulent regimes (Beek, 1965; De Nevers, 1968; Freedman and Davidson, 1969; Hills, 1974; Rietema, 1982). A similar circulation flow pattern has also been reported in other types of three-phase contactors such as liquid-liquid spray columns (Yoshitome and Shirai, 1970; Van der Akker and Rietema, 1979), gas fluidized beds (Lin et al., 1985; Whitehead, 1985), liquid fluidized beds (Latif and Richardson, 1972; Agarwal et al., 1980), and gas-liquid-solid fluidized beds (Fan et al., 1992). Generally, the gross circulation flow field comprises an upward flow in the column core and a downward stream along the wall. This nonuniform velocity distribution is significant in characterizing the bed hydrodynamics, phase mixing characteristics and heat and mass transfer. The success in designing reactor systems lies in comprehensive understanding of the bed hydrodynamics and transport properties. Although theoretical and experimental studies concerning the circulation flow field in three-phase systems are extensive, precise flow structures and governing mechanisms are still not well understood.

The two-dimensional (2-D) systems have been employed to yield important qualitative information in gas-liquid systems (Chen et al., 1989; Tzeng, 1991). In some cases, the 2-D studies have also yielded important quantitative flow information, such as gas bubble wake dynamics in liquid and liquid-solid suspensions (Fan and Tsuchiya, 1990), which is compatible to that in the three-dimensional (3-D) systems. Thus, to explore the complex macro- or microflow structure of the bubble column systems, it is desirable to examine its 2D behavior first.

In this study, pertinent literature on the flow structure in bubble columns and gas-liquid-solid fluidization systems is reviewed. Experiments are conducted in a 2-D column to explore the dynamic macroscopic flow structure of both bubble

Correspondence concerning this article should be addressed to L.-S. Fan.

columns and three-phase fluidization systems. The flow structures, including instantaneous flow patterns and associated bubble and particle dynamics, in these systems are identified via visualization. In addition, two simplified flow conditions, that is, single bubble and single bubble chain flows, are studied to examine a possible formation mechanism for the gross liquid or liquid-solid circulation pattern. The effects of gas and liquid flow rates, and particle properties on the macroscopic flow behavior are studied. Note that all the gas or liquid velocities described here refer to the superficial velocities unless otherwise noted.

Literature Review

Single-bubble-chain flow

Among the earliest studies of liquid circulation in bubble-driven flow is the work of Crabtree and Bridgwater (1969) on the circulation phenomena of a tall column induced by a single bubble chain injected from the column center. The axial velocity profile and pressure difference of the bubble induced liquid motion in a batch system were measured. A steady-state, one-dimensional force balance equation was also developed to account for flow properties. They assumed that the force exerted by a bubble chain on the bubble-surrounding liquid is equivalent to that exerted by a circular rod of a certain characteristic radius moving steadily upward along the axial direction. The predicted liquid axial velocity profile compared fairly well with the experimental data. The detailed flow mechanism and the possible implication of the model for the multiinjector conditions, however, were not given. Extending Crabtree and Bridgwater's (1969) work with inclusion of the wake effects caused by the bubble motion, Miyahara et al. (1984) developed a modified model for liquid circulation induced by a single bubble chain. Although a very simplified wake theory was adopted in Miyahara et al.'s (1984) model, the comparison of the prediction showed a significant improvement over Crabtree and Bridgwater's (1969) model signifying that the bubble wake phenomenon is one of the key factors for the induced liquid flow.

Multiple-bubble-chain flow

Freedman and Davidson (1969) studied the liquid circulation induced by bubbles injected through multiple injectors. In a shallow, two-dimensional bubble column ($1 < H/D < 2$) with air injected from central part of the column at a relatively low gas flow rate, they observed the "gulf stream" phenomenon and postulated the existence of a pair of symmetrical liquid circulation cells. Their postulated circulation structure consists of a bubbly upward flow in the column core region and a bubble-free liquid downward flow region near the sidewall. Using the stream function approach for inviscid liquid motion, they developed a model based on a simplified global force balance and predicted the shape of the "bubble envelope" from the model. While the comparison of the predicted and observed shapes of the bubble envelope appears to be satisfactory, the liquid circulation patterns are not distinctly evidenced in their experimental observation.

More studies, either experimental or theoretical, evolved on the liquid circulation induced by free bubble motion after Freedman and Davidson's (1969) work. These studies involved mostly tall (slurry) bubble columns with the flow field overwhelmingly assumed to be one-dimensional and time-invariant (Rietema and Ottengraf, 1970; Hills, 1974; Ueyama and Miyachi, 1979; Kojima et al., 1980; Walter and Blanch, 1983; Ulbrecht et al., 1985; Yang et al., 1986), although the flows are generally identified to be dynamic and multidimensional in nature (Franz et al., 1984). The experimental measurements of the time-averaged axial velocity profiles used to verify the modeling work were conducted using a point measurement instrument (such as Pitot tubes). Generally, the data provide a velocity profile of upward flow in the central region and downward flow in the wall region. However, the flow structure of upward flow in the wall region and downward flow in the central region was reported to exist in (slurry) bubble columns or gas-solid fluidized beds (Lin et al., 1985; Devanathan et al., 1990). The location with zero liquid velocity, the flow inversion point, is commonly obtained indirectly through interpolation of the radial velocity profile (Hills, 1974). Yang et al.'s work (1986) is one of the few which directly obtained the flow inversion point experimentally by measuring the electrical conductivity of a sodium chloride solution used as the liquid tracer. The flow inversion point is reported to be located at around 0.7 radius for water and 0.5 radius for viscous liquids (Ulbrecht et al., 1985).

Experimental studies

The representative example of the early experimental work on quantitative measurements of axial velocity distribution was that of Hills (1974). In his work, a modified Pitot tube was used to measure both the mean and fluctuating velocities of the liquid circulation induced by the bubble motion. In his work, a conductivity method was incorporated for measuring the gas holdup distribution. While his data were obtained from an intrusive time-averaged point measurement instrument, they have been widely adopted as a data source for model verification.

The liquid-phase mixing rate in bubble columns was reported to depend on the liquid rheological properties by Ulbrecht and Baykara (1981). For low superficial gas velocities (< 0.2 cm/s) and low gas holdups ($< 10\%$), they concluded that the dependence of liquid rheological properties on the mixing rate can be described in terms of the dependence of mixing time on liquid velocities in the central plume region. The significance of the nonuniform velocity and holdup distributions was revealed in their work.

Modeling studies

Mathematical modeling of bubble-induced liquid circulation based on the mass and momentum balance was conducted by Rietema and Ottengraf (1970). In this model, the circulation flow field was divided into two distinct regions: the uniformly distributed bubble street and the bubble-free annular region. It is assumed that the bubble street region is uniform in gas holdup with a constant slip velocity and no bubble coalescence. The turbulent effect was neglected in the model. A criterium concerning minimum energy dissipation was incorporated to close the equations. The model is valid only at very low gas flow rates when the assumptions of laminar flow, bubble-coalescence-free and minimum energy dissipation are held.

Based on a very simplified one-dimensional momentum

equation, Ueyama and Miyauchi (1979) circumvented the unrealistic sharp change of gas holdup at the interface of bubble and annular regions employed in the model of Rietema and Ottengraf (1970) by using the continuous gas holdup correlation developed by Kato et al. (1975). The flow field was assumed to be a turbulence-dominant flow. A universal velocity profile for a single-phase turbulent flow was adopted for the wall region. Their model relied on many empirical coefficients whose physical meanings and numerical values were yet to be determined.

Utilizing the single-phase turbulent mixing length approach with an empirical gas holdup profile, Clark et al. (1987) also employed the one-dimensional turbulence-dominant model to account for the circulation flow pattern in bubble columns. While the predicted axial velocity profile compared fairly well with Hills' (1974) data, the adoption of isotropic turbulence concept and the empirical turbulence equation for single-phase flow remains questionable. It has been shown that the turbulence structure in such a bubble-driven flow is oriented by bubble rising patterns (Franz et al., 1984). By specifying the "saddle-shaped" gas holdup profile in the model, Clark et al. (1987) were able to simulate a circulation pattern with liquid rising along the wall and descending in the central region. The importance of the gas holdup profile in determining the circulation pattern is evident.

Anderson and Rice (1989) introduced a flow field consisting of three zones (core, buffer and bubble-free wall layer) for the bubble column. The momentum equations for both phases employed by Rietema (1982) were adopted in their model. To describe the turbulent effect, von Karman's mixing length hypothesis was used for the core zone and Prandtl's mixing length hypothesis was used for the buffer zone. Note that the flow field of the wall region was considered to be laminar, and the gas holdup was assumed to be constant in either the core or the buffer region. A balance of mass and energy was used to close the equations. In the energy balance, the energy was considered to be mainly dissipated due to the overall velocity profile and the bubble movement. The comparison between their prediction and Hills' data was fairly good. Rice and Geary (1990) and Geary and Rice (1992) proposed modified models with improvements over the assumptions of the number of prevailing flow regions, gas holdup distribution, turbulent mixing length and viscous effect, while retaining the assumption of the existence of one pair of symmetric circulation cells. Their model yields good predictive capability in the approach using the one-dimensional concept although the flow field may actually consist of multiple pairs of nonsymmetric circulation cells.

Instead of momentum balance equations, Whalley and Davidson (1974) employed an energy balance equation, which accounts for the energy dissipation due to the presence of bubble wakes and the hydraulic jump raised by the rising bubbles at the liquid surface, with the vorticity equation to calculate the velocity field in shallow bubble columns. The flow structure was also assumed to consist of one pair of circulation cells. In their model, the validity of the application of Lamb's vorticity equation, which was derived for an inviscid fluid in axisymmetrical single-phase flow, to turbulent three-phase flow with a viscous liquid was not justified.

Joshi and Sharma (1979) argued that the liquid circulation velocities calculated by the energy balance method are closer to reality than those predicted by the momentum balance method. Therefore, a modified model was developed by them closely following the work of Whalley and Davidson (1974). Instead of one pair of circulation, Joshi and Sharma (1979) proposed a circulation structure of multiple stationary cells. These cells were axisymmetrically located in the axial direction with the cell height equal to the column diameter. The proposed circulation structure results in the flow between adjacent cells along the axial direction to flow in opposite direction, which violates the natural flow phenomena in which no two different flow directions can exist at the same location and the same time. Joshi (1980) improved this model by assuming an interacting cell structure. The predicted time-averaged velocity profile compared reasonably well with Hills' data. However, the underlying assumption of the structure of the circulation cells in their work remains to be clarified.

Flow structure studies

By applying hot-film anemometry (HFA), Franz et al. (1984) measured the "instantaneous" axial, tangential and radial liquid velocities in a three-dimensional bubble column. Through the point measurements over a period of time, the "instantaneous" velocity and turbulence intensity profiles along the different directions were obtained. They concluded that the "instantaneous" liquid velocity profiles were generally asymmetrical and of dynamic nature. The axial turbulent intensity was significantly higher than those in radial and tangential directions. The radial and tangential turbulent intensities were rather uniform in the radial direction, and in contrast, the axial intensity varies significantly. A region of the largest axial turbulent intensity was identified to be in-between the central upward flow (that is, bubble street) and downward flow near the wall. From their test results, a structural flow model comprising three zones was postulated, where a bubble street (generating swarm turbulence) with step upward helical flow located in the central zone associated with a downward flow annular zone and the vortex street of anisotropic turbulence located between the above-mentioned two regions. The work is important as it provides experimental evidence regarding the dynamic nature of the flow structure.

Recently, Devanathan et al. (1990) adopted the radioactive-particle-tracking technique developed by Lin et al. (1985) for gas-solid fluidized beds to obtain the liquid flow fields in a three-dimensional bubble column. The time/volume-averaged velocity field was obtained through the tracing of a radioactive particle. Their results suggested the existence of a pair of circulation cells with the liquid descending along the wall and ascending in the central region for gas velocities greater than 0.05 m/s. At lower gas velocities, however, two pairs of cells appeared; the lower cell pair located in the entry region are of liquid ascending along the wall and descending in the central region. A similar flow pattern (two pairs of circulation cells) was reported by Lin et al. (1985) for the gas-solid system. Devanathan et al. (1990) indicated the important dependence of flow patterns on the gas flow rate. It should be noted that the circulation structure reported by Devanathan et al. (1990) was based on the velocity profiles obtained using the time and modified ensemble averaging. Thus, this flow structure does not represent the instantaneous one observed in the system.

It is apparent that more studies leading to better under-

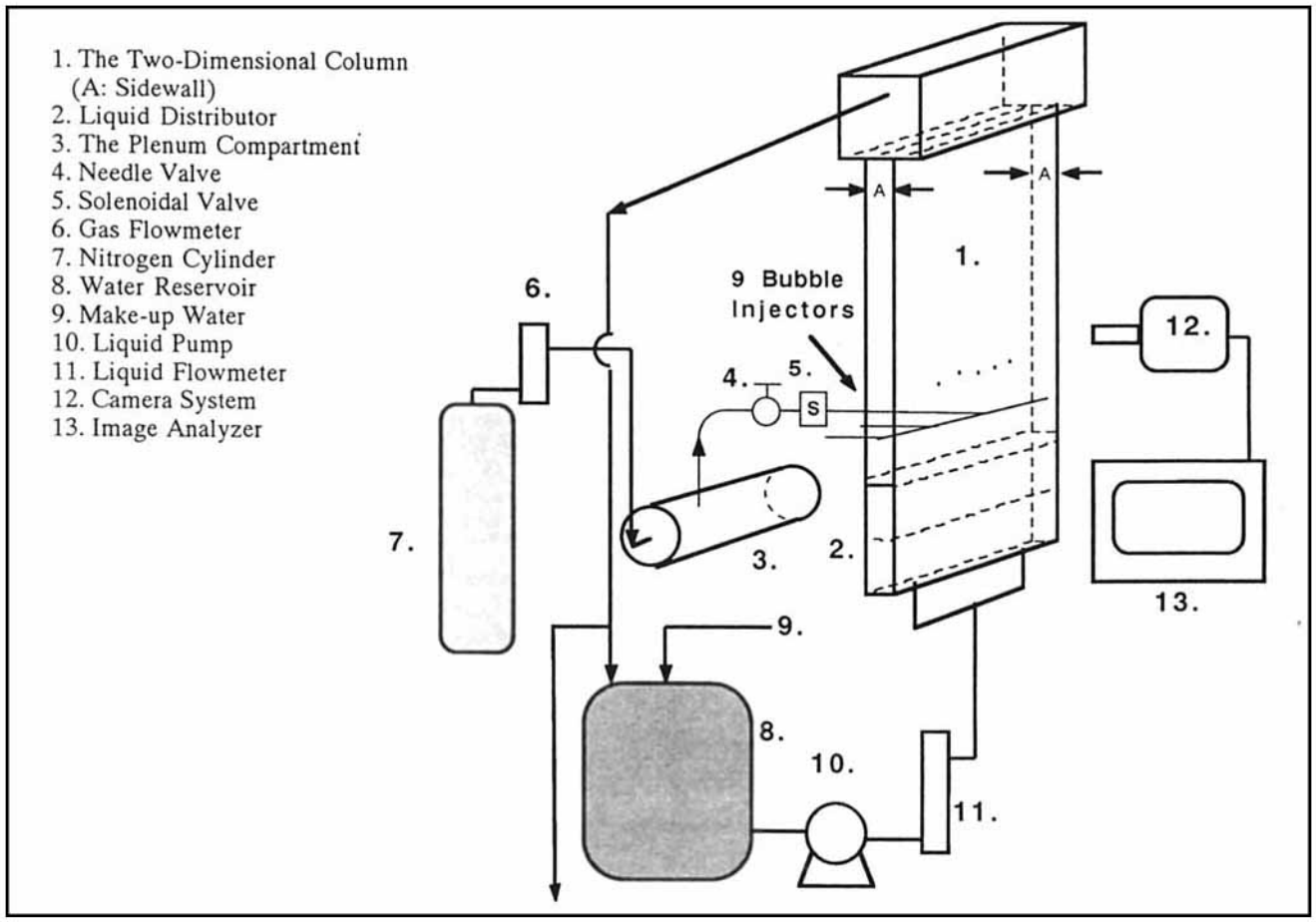

Figure 1. Two-dimensional fluidized bed.

standing and prediction of the flow structures of the bubble columns and three-phase fluidized beds are necessary. Specifically, the dynamic circulation structure in these systems needs to be explored further.

Experimental

Tap water is used as the liquid phase. Four types of particles including 163-μm and 326-μm glass beads ($\rho_s = 2.5$ g/cm^3), 300-μm activated carbon particles ($\rho_s = 1.5$ g/cm^3), and 1.5-mm acetate beads ($\rho_s = 1.25$ g/cm^3) are used as the bed particles. Pure nitrogen gas is used as the gas phase. The gas velocities employed in this study vary from 5 mm/s to 64 mm/s. The gas pressure is maintained within 10 and 12 psig (69 and 83 kPa) upstream of the gas plenum. Neutrally buoyant particles as the liquid tracer are 140–160-μm colored Pliolite particles. To ensure that the seeding particles follow the flow closely and have virtually no effects on the flow structure, the concentration of the seeding particles is maintained below 0.1% and the Stokes number of the seeding particles is much smaller than 1. The liquid or particle flow patterns are recorded by video and by cinemaphotography.

Figure 1 shows the experimental apparatus employed in this study. The two-dimensional fluidized bed is made of Plexiglas. The viewing section of the bed is 0.483 m in width, 1.6 m in height, and 12.7 mm in depth. Below this section is the liquid distributor which consists of a packed particle section and a liquid calming section. The gas distributor is made up of nine tube injectors flush-mounted on the side. The injector opening is 0.16 mm ID. The gas flow through each injector is individually regulated by a solenoid valve and a needle valve and is connected to the plenum compartment outside of the bed. Most of the experiments are conducted with even distribution of gas flow through all injectors. Specific experiments are performed with injector blockage to study the effect of inlet gas flow distribution on the bed flow structure. The distance between two adjacent bubble injectors is 50.8 mm, and that between the end injector and the sidewall is 38.1 mm. The plenum is connected to a nitrogen cylinder with a dual-pressure regulator. These bubble injectors are positioned 100 mm above the top of the particle packing section of the liquid distributor. The particle disengagement section is located at the top of the viewing section. The effluent liquid stream is recycled back to a reservoir, where the liquid temperature is maintained within 20–22°C for all experiments.

Results and Discussion

At a low gas velocity, no apparent gross circulation can be observed and the bubbles rise rectilinearly in the bubble column or three-phase fluidized bed. As the gas velocity reaches a certain value, denoted as the critical gas velocity, the trajectories of the bubbles injected near the sidewalls start to deviate

from the rectilinear pattern, while in the bed center, trajectories of bubbles remain fairly rectilinear. Note that the sidewalls in this text refer to the 12.7-mm-wide walls as noted in Figure 1. Meanwhile, descending vortices (local circulation cells) start to form in the region near the sidewall. A noticeable amount of the liquid descends via the descending vortices as well as along the proximity of the sidewalls, where the liquid or slurry phase continuously flows downward. In the column center, dynamic formation of vortices takes place between two neighboring bubble streams. The bed structure with such multiple vortices in the bed transverse direction resembles that proposed by Bhavaraju et al. (1978) for gas sparging through viscous liquids. The critical gas velocity is about 4–6 mm/s for the two-dimensional gas-liquid system under the liquid-batch condition and depends on the liquid velocity and properties of bed particles for a three-phase fluidization system. It is noted that even though the bubbles near the sidewalls start to migrate away from the sidewalls at the critical velocity, some bubbles move in clusters and there is no bubble coalescence observed: that is, the migration of the bubbles and the subsequent formation of the four flow regions (to be discussed later) take place even before the occurrence of bubble coalescence.

With a further increase in the gas velocity, the lateral migration distance of the bubbles near the sidewalls and the size of vortices increase. Consequently, the distance between two neighboring bubble streams decreases, and eventually bubble-bubble interactions occur. Development of multiple vortices in the transverse direction is thus impeded. While there are always multiple vortices in the area near the sidewalls, the bed structure can generally be described as being of the gross circulation pattern with an upward liquid (or liquid-solid) flow in the column center and descending streams along the sidewalls. As the gas velocity increases beyond the transient velocity which is about 9 mm/s, bubble coalescence and break-up take place intensively and the flow enters the churn-turbulent regime. Note that the observed transient velocity from the bubbly to the churn-turbulent (coalesced bubble) regimes in the 2-D column (about 9 mm/s) is lower than that of a 3-D column (about 2–4 cm/s as noted by Tsuchiya and Nakanish, 1992). Apparently, this is due to the less degree of freedom in the bubble movement in the 2-D column compared to the 3-D column.

Multiple vortices along the sidewalls are developed steadily. As shown in Figure 2, vortices are formed at the sidewalls for the gas and liquid velocities of 0.774 cm/s and 0.103 cm/s, respectively. The behavior of these vortices is of a dynamic nature and the formation of the vortices at each sidewall appears to be independent of each other at relatively low gas velocities. The cells become staggered, however, as the gas velocity increases. Similar staggered multiple-vortex structures have also been reported by Chen et al. (1989) in a bubble column with an aspect ratio larger than 1, although no detailed flow characteristics and formation mechanism were provided by them.

Macroscopic flow structures

To generalize the above observations, the gross bed circulation structure for gas-liquid and gas-liquid-solid systems can be represented by four distinct flow regions based on the local liquid flow characteristics and bubble dynamics. These regions,

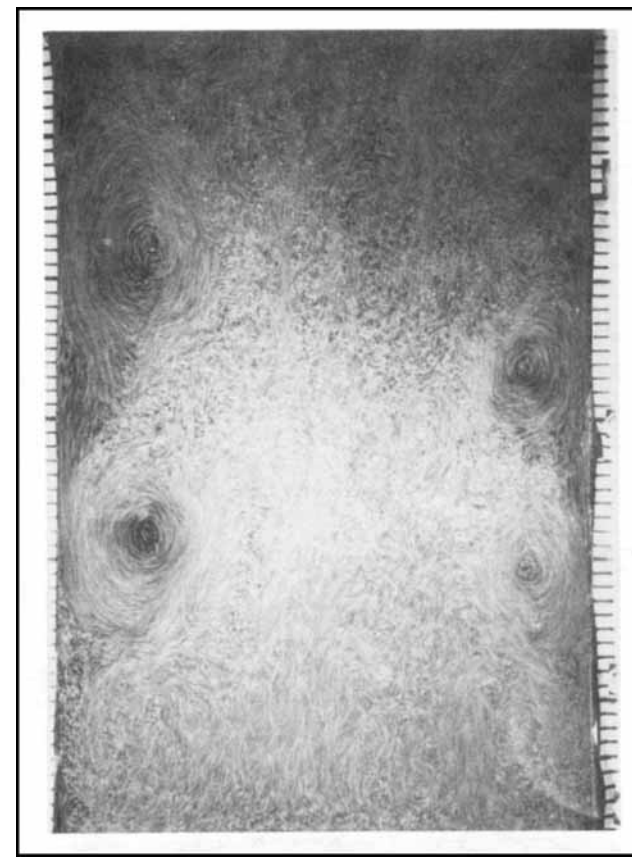

Figure 2. Flow field of a gas-liquid-solid fluidized bed containing 1.5-mm acetate particles for $U_g = 0.774$ cm/s and $U_l = 0.103$ cm/s.

namely descending flow, vortical flow, fast bubble flow, and central plume regions, in the order from the sidewalls, are described in the following sections. The flow structure is shown in Figures 3 and 4.

Descending Flow Region. This region represents the area adjacent to the sidewalls where the liquid phase flows downward. At low gas velocities, this region is free of bubbles. At relatively high gas velocities, small bubbles are observed in this region and they can be either stationary or mobile depending on the bubble sizes and the descending liquid velocity. The descending velocity, however, is rather dynamic as most of the bubbles in this region are observed to move up and down. The dynamic nature of this region is related closely to the formation and movement of vortices nearby (that is, in the vortical flow region as discussed below).

Vortical Flow Region. Adjacent to the descending flow region is the vortical flow region characterized by the existence of moving (primarily descending) vortices. Vortices form steadily near the free bed surface. It is observed that vortices descend relatively steadily along the sidewalls at low gas velocities. As the gas velocity increases, vortices become rather unstable due to disturbances caused by small bubbles trapped in the cells and by large bubbles rising in the neighboring fast bubble flow region. The descending vortices will deform and eventually disappear after traveling over some distance; the

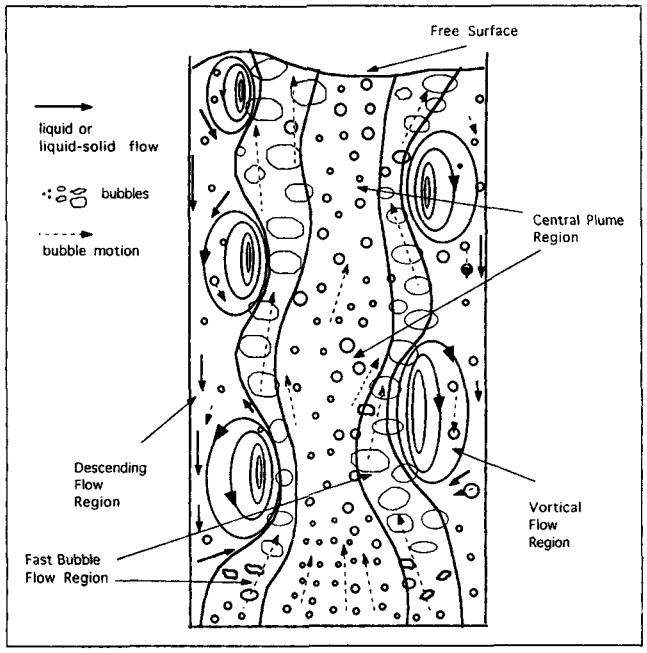

Figure 3. Classification of regions accounting for the macroscopic flow structure.

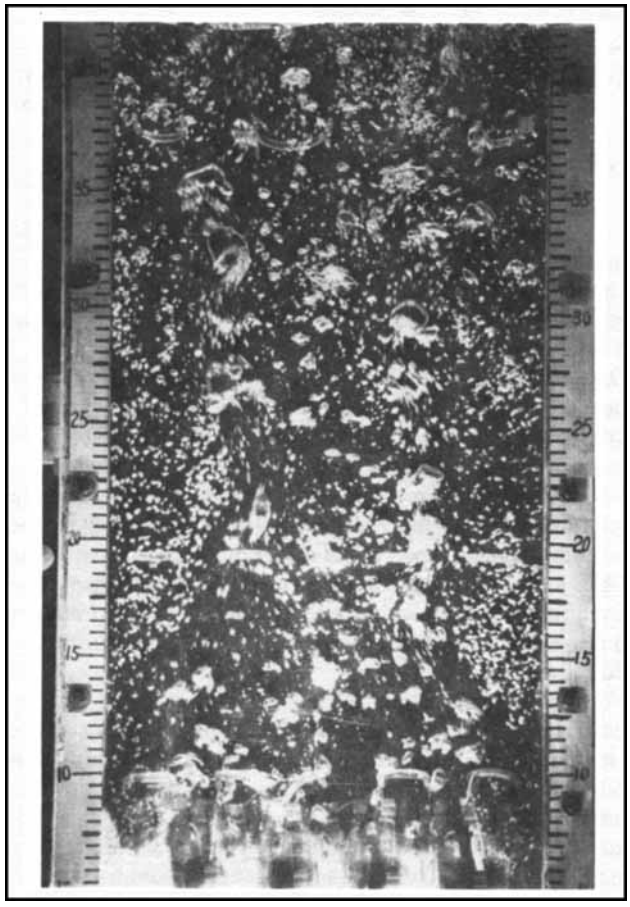

Figure 4. Flow field of a gas-liquid system for $U_g = 3.87$ cm/s and $U_l = 0$ cm/s.

deformation often yields new vortices in the nearby downward stream.

The velocities of vortices descending along the sidewall depend on the operating conditions, such as gas and liquid velocities. Under the operating conditions considered in this study, the vortices are observed to be prolate ellipsoid in shape. The boundary of a vortex can be identified by the outermost closed loop of tracer trajectories, and the size of a circulation is herewith defined as the lateral length of the boundary. Figure 5 shows the variation of the vortex size of a liquid-batch system with respect to the gas velocity. The vortex size increases with the gas velocity up to the bubbly-churn turbulent transient velocity (9 mm/s), beyond which the vortex size becomes constant (about 17 cm). The value of this constant vortex size is believed to depend strongly on the geometry of the column; further investigation is required to verify this point.

Fast Bubble Flow Region. This region is located between the vortical flow region and the central plume region, and is characterized by cluster bubbles at relatively low gas velocities or relatively high velocities by coalesced bubble moving at high velocities. The coalesced bubble flow is typically noted for the churn-turbulent region. The bubble clustering or coalescence is caused by the migration of bubble chains near the sidewalls promoted by the presence of the vortices near the gas distributor in the vortical flow region. The bubble coalescence occurs when the vortices are large and neighboring bubbles are sufficiently close. Note that the gas velocity required for transition from clustered bubbles to coalescence bubbles also depends on the extent of contamination of the liquid medium (Fan and Tsuchiya, 1990). The existence of wakes of these large bubbles induces acceleration of the nearby trailing bubbles forming even larger bubbles at the upper part of the bed. These fast-moving bubble-coalesced streams rise up in a wavelike manner. The wavelike bubble movement in this region intensifies the formation and the motion of vortices in the vortical flow region. This liquid vortical flow motion, however, also enhances the wavelike motion of the fast bubble stream. The vortices are confined between the sidewalls and the concavity of the fast-moving bubble-coalesced streams. In another way, the

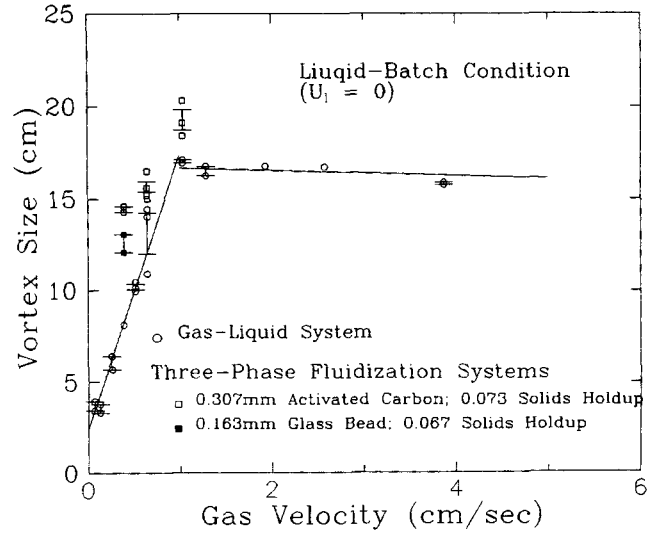

Figure 5. Variation of the vortex size with the gas velocity under the liquid-batch operation mode.

vortices are squeezed and then either decimated or pushed down along the descending flow region between sidewalls and convexity of coalesced bubble streams. Through the use of both visualization and full-field measurement techniques (Chen and Fan, 1992), this wavelike motion in the 2-D column is verified to translate into a spiral motion in the 3-D column as observed by Reese et al. (1992).

In the fast bubble flow region, bubbles are larger and rise faster than those in the central plume region (to be discussed later). In addition to coalescence, bubble break-up due to the local flow disturbance or turbulent stress takes place more significantly in this region than in the central plume region. Through observing the tracer particles and colored bed particles in the flow field, very little direct mass exchange is observed between the bubbly upward flow region and the vortical flow region except through the top and bottom of the fast bubble flow region, especially when the gas velocity is high. This observation implies that the fast bubble flow region serves as a baffle on the radial mass transfer for both the solid and liquid phases. This is because the axial liquid velocity in the fast bubble flow region is so large that the bed particles and liquid elements are essentially moving also axially. When the gross circulation is established, the fast bubble flow region dictates the macroscopic flow structure of the system.

Central Plume Region. The central plume region is in the column center and is surrounded by the fast bubble flow region. In this region, the distribution of bubble sizes is relatively uniform with less bubble-bubble interaction compared to those in the fast bubble flow region. At high gas velocities, the bubble chains in this region also move in a wavelike movement and swing laterally back and forth over almost the entire bed width. Such a swinging phenomenon is observed to synchronize with the wavelike bubble movement in the fast bubble flow region. The liquid is observed to flow downward in the region between each bubble chain under low gas flow rates. No such downward liquid flow pattern, however, has been observed for high gas flow rate conditions.

At a relatively low gas velocity (but larger than the bubbly-churn turbulent transient velocity), the bubble-bubble interactions in the central plume region are not noticed despite the occurrence of significant bubble coalescence in the fast bubble flow region. Vortices form between two adjacent bubble streams, but their presence is only transient and their movement is rather random. On the other hand, at a high gas velocity, vertical bubble coalescence takes place which differs from lateral, coalescence-dominated bubble-bubble interaction in the fast bubble flow region.

Mechanisms for gross liquid circulation

It is revealed that the occurrence of the gross liquid circulation is closely associated with the movement of the fast bubble region which is governed by the bubble coalescence due to the lateral migration of the bubbles near the sidewalls. Studies on bubble dynamics near the sidewalls are therefore essential to the fundamental understanding of the formation mechanism of the gross circulation encountered in bubble columns and three-phase fluidized beds. The mechanisms of the formation of circulation flow patterns can be deduced in part through observing the movement of a single bubble near sidewalls and trajectory of a single bubble chain in a liquid batch system.

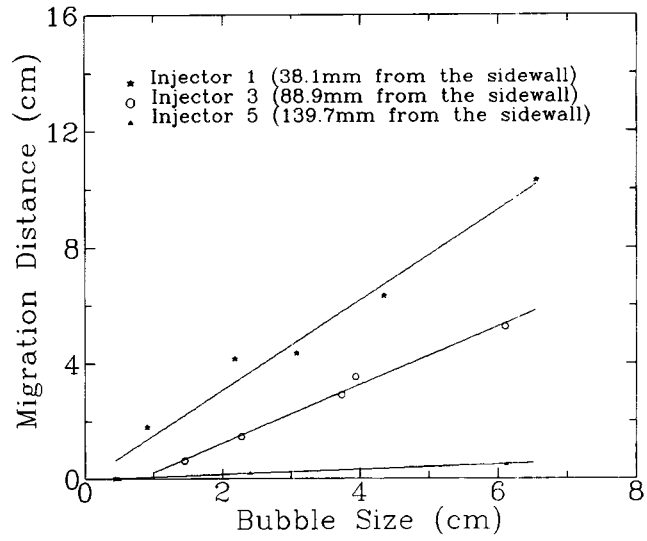

Figure 6. Relationship between the maximum bubble migration distance and the bubble size for a single bubble rising in a stationary liquid medium.

Bubble Lateral Migration Near Sidewalls. As a single bubble rises near a vertical wall in a stationary liquid medium, a secondary motion in the horizontal direction is observed. The bubble rises rectilinearly right after injection from the bubble injector and then moves away from the sidewall at a relatively constant lateral velocity after a short distance above the injection point. Figure 6 shows the variation of the maximum migration distance of a single bubble injected from different location with the bubble size. It shows that the migration distance and the velocity increase with the bubble size. For a given bubble size, however, the migration distance and the velocity increase when the bubble injector is closer to the sidewall. The migration distance is defined as the lateral deviation distance of the actual bubble path from the vertical axis of the bubble injector. The migration velocity is calculated from the migration distance and elapsed time. It is also found that the migration velocity of a bubble is relatively constant with axial positions except at the top or the bottom of the bed.

The lateral migration of a single bubble is a result of flow boundary, that is, the sidewalls. Since the distance from the bubble to each of the two sidewalls is different, the liquid momentum transferred from the rising bubble is dissipated at uneven rate. This uneven dissipation rate of momentum yields an asymmetric liquid velocity profile to the bubble center and results in a higher pressure at the side closer to the sidewall. This lateral pressure difference causes the migration of a large bubble away from the sidewall. For a smaller bubble, however, the bubble-driven liquid flow is relatively small and thus the resultant pressure difference is small. The migration effect of a small bubble is then insignificant. The lateral pressure difference and hence the migration effect of the bubble also become less significant when the bubble injector is located further away from the sidewall.

It is found in this study that the onset of the gross circulation structure in a multibubble system is initiated by the lateral migration of bubbles near the sidewalls. At a high gas velocity, the bubble front near the sidewalls in a multibubble system

migrates away from the sidewall according to the migration mechanism for a single bubble in stationary liquid. A bubble-free area along the sidewalls is then created. The liquid (or liquid-solid mixture) in the bubble-free area has to flow downward to counterbalance the ascending flow induced by rising bubbles in the column center. The lateral migration of bubbles results in the bubble coalescence and the creation of the fast bubble flow region which aids to strengthen the vortical flow and descending flow regions. A gross circulation structure is then established. At a low gas flow rate, on the other hand, the gross circulation cannot be established due to inadequate bubble migration from the sidewalls. Since bubble sizes are determined by various factors including the gas flow rate, the bubble injector size, and the distance between injectors for a given flow medium, these factors also dictate the onset of the gross circulation in bubble columns and three-phase fluidized beds.

Circulation Induced by a Bubble Chain. The trajectory of a single bubble chain injected near the sidewall in a batch liquid system is observed to differ significantly from that of a single bubble. Bubbles in such a bubble chain first rise with lateral migration toward the sidewall as shown in Figure 7 which provides the typical flow structure of a single bubble chain. As bubbles approach the bed surface, their upward movement is hindered due to the presence of a vortex at the bed surface corner. The bubbles thus sharply change the path and move toward the column center. The formation of the vortex existing at the bed surface is apparently due to the secondary flow caused by the end zone effect.

The liquid flow induced by a chain of bubbles exhibits a gross circulation pattern with upward flows near the bubble chain locus and downward flows along the sidewalls. Bubble paths are observed to follow part of the liquid circulation boundary closely. The locus of the bubble stream does not swing as observed in systems with multiple bubble chains after the flow circulation is fully developed which implies that the bubble motion is dictated by the fully developed circulation pattern. Such a steady circulation pattern generally is not seen in systems with multiple bubble chains where perturbations generated by bubble migration and coalescence are substantial.

The gross liquid circulation occupies almost the entire area between the bubble chain locus and the far-sight sidewall. There is an apparent liquid stagnation region inside the circulation cell. The stagnation region, however, is not located at the geometric center of the cell. The eccentric cell configuration does not resemble that assumed by Freedman and Davidson (1969) or Hill's spherical vortex (Hill, 1894). Furthermore, velocity gradients appear to be larger in the proximity of the bubble chain than near the sidewall. This is due to the fact that the upward liquid flow is induced primarily by bubble wake carriage (Tang and Fan, 1989) and drift-induced by bubble rise (Tsuchiya et al., 1992). The liquid flow, while induced, acquires momentum mainly in the primary wakes of rising bubbles. Through the roll-up and shedding phenomena of bubble wakes (Fan and Tsuchiya, 1990), momentum is transferred from the primary wakes to the surrounding liquid. Consequently, the induced liquid flow field exists only in the close proximity of a single bubble chain. The underlying momentum transfer mechanism governing the annular descending stream differs inherently from that of the central upward stream, since the momentum of the descending liquid stream along the sidewalls is transferred through the liquid viscosity and dissipated primarily at the wall. Therefore, the one-dimensional momentum equation without taking into account the bubble wake effects does not describe such flow fields induced by bubbles.

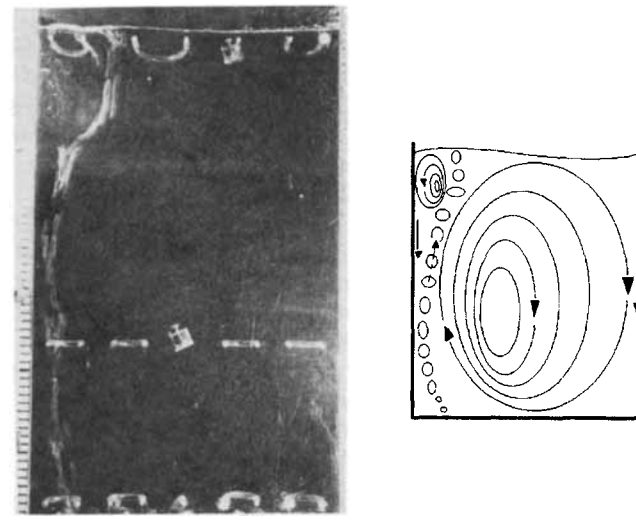

Figure 7. Flow field induced by a single bubble chain in a liquid-batch system ($U_g = 0.769$ cm/s and $U_l = 0$ cm/s).

Effects of liquid velocity

Figure 8 shows the relationship between the vortex size and the liquid velocity of a bubble column and three-phase fluidized beds containing 163-μm glass beads and 300-μm activated carbon particles, respectively. The vortex size increases initially with the liquid velocity to a maximum value and then decreases

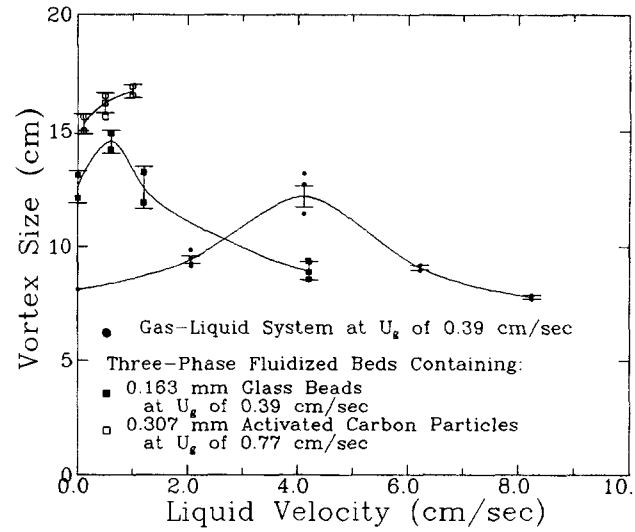

Figure 8. Variations of the vortex size with the liquid velocity in a bubble column and three-phase fluidized beds for 0.163-mm glass beads and 0.30-mm activated carbon particles.

with further increase in the liquid velocity. The data for three-phase fluidization shown in Figure 8 are limited due to the small in-bed region caused by column height limitation under prescribed gas and liquid flow velocities. The small in-bed region impedes the flow visualization to be conducted adequately. The relationship between the vortex size and the liquid velocity in three-phase fluidized beds appears to be similar to that of bubble columns. At a low liquid flow rate, the inertia of the uniform inlet liquid flow stream near the sidewalls is not sufficiently strong compared to that of lateral movement of liquid flow caused by the migration motion of bubbles or the existing gross circulation motion. Therefore, the inlet liquid stream near the sidewalls follows the existing lateral motion toward the bed center. The vortices are then strengthened, and hence the liquid circulation rate is enhanced with an increase in the liquid velocity. On the other hand, at a high liquid flow rate, the inertia of the inlet liquid flow stream is strong enough to retard the liquid downward flow near the sidewalls and therefore suppress the development of the vortices in the vortical flow region. Consequently, an increase in the liquid flow rate reduces the vortex size. The optimum liquid flow rate for maximum vortex size depends strongly on the operating conditions of a three-phase fluidization system as demonstrated in Figure 8. Since the vortex strength is a function of operating conditions such as gas flow rate, solids holdup, and particle size, the velocity of the liquid required for obtaining the maximum vortex size also varies with these operating conditions.

Particle effects

As noted, four types of particles including 1.5-mm acetate, 300-μm activated carbon, and 163-μm and 326-μm glass beads are used in the experiments. The general gross circulation phenomena in beds of 300-μm activated carbon particles and 163-μm glass beads with solids holdup up to 25% are found to be similar to those observed in bubble columns. Thus, the general macroscopic flow structure for these systems can be represented by that for bubble column systems described earlier, although the vortex sizes and descending velocities in these systems may deviate under similar operating conditions (see Figure 5). The deviation is due to the change in the rheological properties of the mixture and hence the energy dissipation rate when the solid particles are present.

For the bed of 1.5-mm acetate and 326-μm glass beads, a gross circulation pattern is not evident at the solids holdup above 0.2 (see Figure 9). Beside the change of mixture rheological properties, the particle inertia effect becomes important and retards the development of vortices at high solids holdup conditions. Instead of global particle circulation as described for bubble columns, the in-bed structure consists of several particle vortices in the transverse direction where bed particles are driven upward by bubbles along with the bubble streams and slowly fall down between two bubble streams. Such a bed structure resembles that proposed by Bhavaraju et al. (1978). For all operating conditions considered in this study, although the circulation flow pattern in the in-bed region does not appear for high solids holdup cases, one pair of vortices are always observed in the freeboard region where the solids holdup is substantially low (see Figures 9 and 10). This observation reflects the effect of the solids holdup on macroscopic flow behavior in a three-phase fluidized bed in that the interaction between solid and liquid phases become significant at high solids holdups.

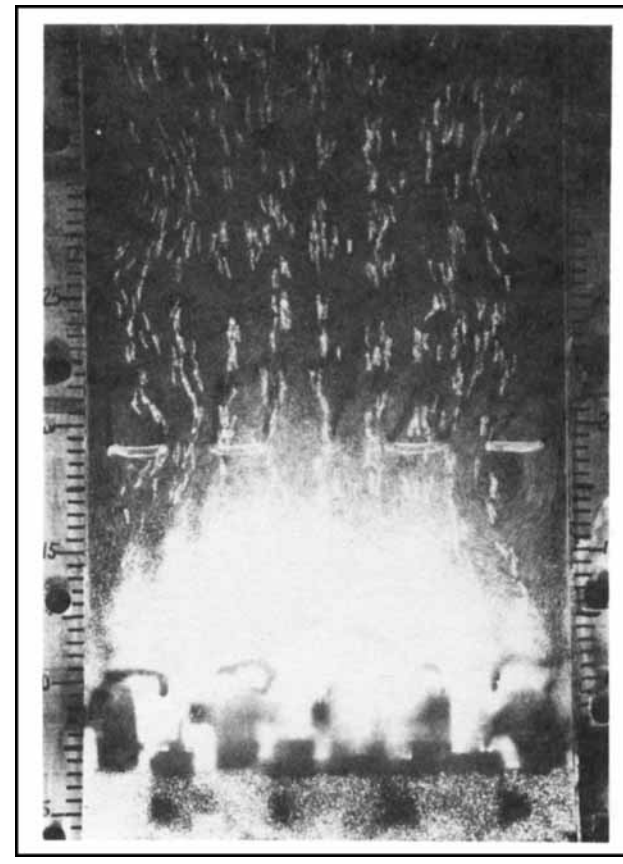

Figure 9. Flow field of a gas-liquid-solid fluidized bed containing 1.5-mm acetate particles for $U_g = 0.645$ cm/s and $U_l = 0.052$ cm/s.

Effects of inlet gas flow distribution

Effects of the inlet gas flow distribution on the macroscopic flow structure are examined. The inlet gas flow distributions are characterized by four different flow conditions established through blockage of gas injectors: (1) blockage of injectors 1 and 9; (2) blockage of injectors 1 and 2; (3) blockage of injector 5; and (4) blockage of injectors 2, 4, 6 and 8. Under this wide range of inlet gas flow variations, it is observed that once the gross circulation is established, the general flow structure given in Figure 3 is valid, although the relative sizes of the four regions may vary. The specific flow behavior characterized by rising bubble dynamics and descending vortical flow for each of these flow conditions is given in the following:

Condition 1. The bed structure under this condition is similar to that without injector blockage. However, the critical gas velocity for the gross liquid circulation at the batch-liquid condition is about 0.8–1.0 cm/s which is greater than that for operation without injector blockage (4–6 mm/s). Since the distance between the sidewall and the nearest bubble injector is longer (8.89 mm), the bubble migration distance is less at a given gas velocities, and hence the interaction between neighboring bubble chains is less significant. A higher gas velocity

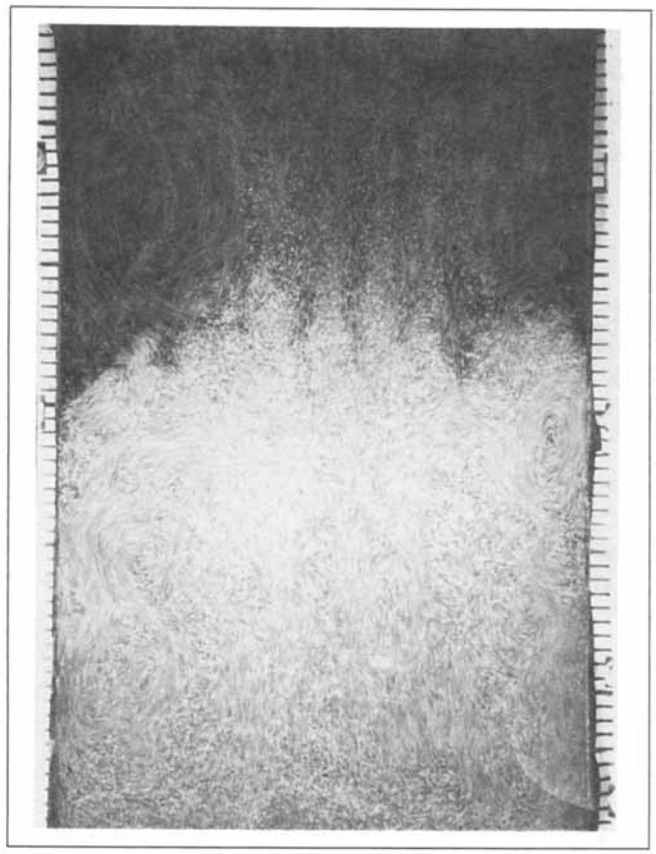

Figure 10. Flow field of a gas-liquid-solid fluidized bed containing 1.5-mm acetate particles for $U_g = 0.774$ cm/s and $U_l = 0.052$ cm/s.

therefore is necessary to promote bubble lateral migration and to start up with the gross liquid circulation.

Condition 2. A stationary vortex forms and resides in the region right above the plugged injectors at all gas velocities

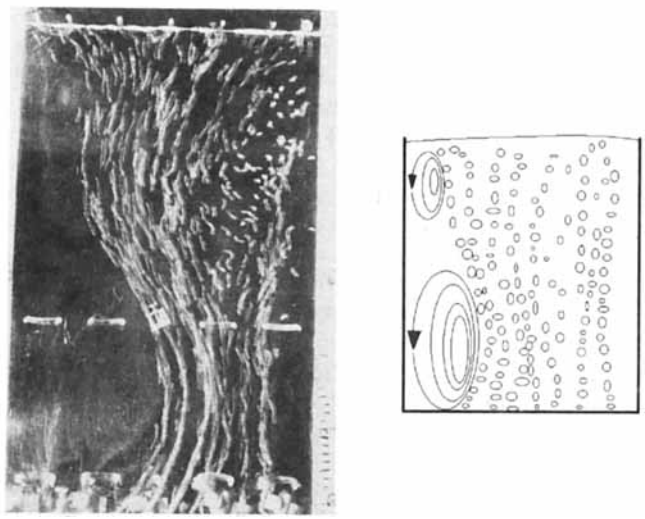

Figure 11. Flow field of a gas-liquid system with blockage of injectors 1 and 2 for $U_g = 0.513$ cm/s and $U_l = 0$ cm/s.

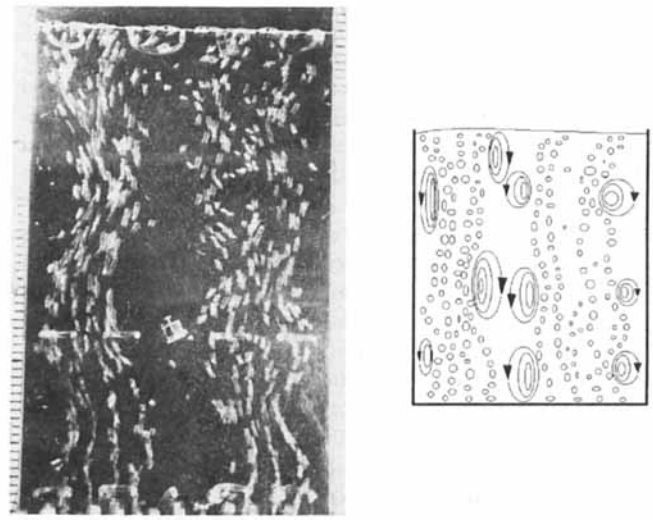

Figure 12. Flow field of a gas-liquid system with blockage of injector 5 for $U_g = 0.636$ cm/s and $U_l = 0$ cm/s.

employed in this study (see Figure 11). The size of the vortex is observed to be fairly time-invariant. It is oval-shaped with the center near the bubble stream. At higher gas velocities, some small bubbles (less than 8 mm in bubble width) are trapped in the vortex for a significant period of time. At the upper part of the bed, vortices of relatively small sizes form and exhibit similar characteristics to those in the vortical flow region of gas-liquid systems with normal bubble injections.

Condition 3. The critical gas velocity is roughly the same as that of the column without injector blockage. The bed consists of two parts separated by a relatively low gas holdup region in the bed center (see Figure 12). The interaction between particles is insignificant under the operating conditions considered. Along the bed central axis where the gas holdup is low, portions of the liquid phase descend and dynamic vortices form. The descending flow region and the vortical flow region are thus significantly reduced compared to those with other distributor arrangements. The outcomes of such inlet flow distribution are that the liquid circulation is less intensive, and the distribution of the radial average gas holdup is fairly uniform.

Condition 4. At relatively low gas velocities, all the bubbles rise fairly rectilinearly with negligible interaction (see Figure 13). Small vortices form and decay randomly between the two adjacent bubble chains. The gross liquid circulation is less intensive compared to those observed in the bed without injector blockage. This is due to the fact that the bubble-bubble interactions between the neighboring bubble chains are insignificant when the bubble injector distance is sufficiently large.

Concluding Remarks

Macroscopic flow structures and mechanisms of liquid circulation in gas-liquid and gas-liquid-solid systems are investigated through flow visualization in a two-dimensional column. Based on the bubble dynamics and local liquid flow patterns, four distinct flow regions are identified when the gross circulation flow field occurs in the system. They are central plume

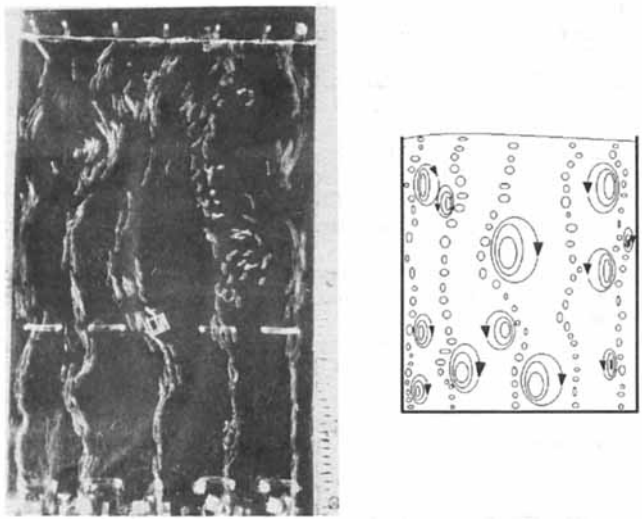

Figure 13. Flow field of a gas-liquid system with blockage of injectors 2, 4, 6 and 8 for $U_g = 0.539$ cm/s and $U_l = 0$ cm/s.

region, fast bubble flow region, vortical flow region, and descending flow region. The holdup distribution of each phase is highly nonuniform resulting from different flow characteristics existing in these regions. Interactions between the fast bubble flow region and the vortical flow region are observed to dictate the instantaneous flow field of the gas-liquid and gas-liquid-solid fluidization systems. The mechanism for the onset of the liquid circulation is found to be due to the lateral migration of bubbles near the flow boundary, that is, the sidewalls of the two-dimensional column. Bed particles with small sizes and/or small density differences with the liquid medium follow liquid trajectories closely, while liquid circulation is retarded by large/heavy bed particles in dense bed conditions. At a low gas velocity, an increase in the liquid velocity tends to suppress the size of the vortical flow region. At a high gas velocity, the liquid circulation rate increases with the liquid velocity. The blockage of the central bubble injector or the increase in distance between the adjacent bubble injectors results in less intensive gross liquid circulation.

Acknowledgment

The work was supported by the National Science Foundation Grant CTS-9200793.

Notation

D = column diameter
d_v = vortex size
H = column height
U_g = gas velocity
U_l = liquid velocity
ρ_s = particle density

Literature Cited

Agarwal, G. P., J. L. Hudson, and R. Jackson, "Fluid Mechanical Description of Fluidized Beds. Experimental Investigation of Convective Instabilities in Bounded Beds," *Ind. Eng. Chem. Fundam.*, **19**, 59 (1980).

Anderson, K. G., and R. G. Rice, "Local Turbulence Model for Predicting Circulation Rates in Bubble Columns," *AIChE J.*, **35**, 514 (1989).

Beek, W. J., "Oscillations and Vortices in a Batch of Liquid Sustained by a Gas Flow," *Symp. on Two-Phase Flow*, **2**, T405 (June, 1965).

Bhavaraju, S. M., T. W. F. Russell, and H. W. Blanch, "The Design of Gas Sparged Devices for Viscous Liquid Systems," *AIChE J.*, **24**, 454 (1978).

Chen, J. J. J., M. Jamialahmadi, and S. M. Li, "Effect of Liquid Depth on Circulation in Bubble Columns: A Visual Study," *Chem. Eng. Res. Des.*, **67**, 203 (1989).

Chen, R. C., and L.-S. Fan, "Particle Image Velocimetry for Characterizing the Flow Structure in Three-Dimensional Gas-Liquid-Solid Fluidized Beds," *Chem. Eng. Sci.*, **47**, 3615 (1992).

Clark, N. N., C. M. Atkinson, and R. L. C. Flemmer, "Turbulent Circulation in Bubble Columns," *AIChE J.*, **33**, 515 (1987).

Crabtree, J. R., and J. Bridgwater, "Chain Bubbling in Viscous Liquids," *Chem. Eng. Sci.*, **24**, 1755 (1969).

De Nevers, N., "Bubble Driven Fluid Circulations," *AIChE J.*, **14**, 222 (1968).

Devanathan, N., D. Moslemian, and M. P. Dudukovic, "Flow Mapping in Bubble Columns Using CARPT," *Chem. Eng. Sci.*, **45**, 2285 (1990).

Fan, L.-S., *Gas-Liquid-Solid Fluidization Engineering*, Butterworth, Stoneham, MA (1989).

Fan, L.-S., and K. Tsuchiya, *Bubble Wake Dynamics in Liquids and Liquid-Solid Suspensions*, Butterworth, Stoneham, MA (1990).

Fan, L.-S., J.-W. Tzeng, and H. T. Bi, "Flow Structure in a Two-Dimensional Bubble Column and Three-Phase Fluidized Bed," *Fluidization VII*, p. 399, D. E. Potter and D. J. Nicklin, eds., United Engineering Trustees, Inc. (1992).

Franz, K., T. Borner, H. J. Kantorek, and R. Buchholz, "Flow Structures in Bubble Columns," *Ger. Chem. Eng.*, **7**, 365 (1984).

Freedman, W., and J. F. Davidson, "Hold-up and Liquid Circulation in Bubble Columns," *Trans. IChemE*, **47**, T251 (1969).

Geary, N. W., and R. G. Rice, "Circulation and Scale-Up in Bubble Columns," *AIChE J.*, **38**, 76 (1992).

Hill, M. J. M., "On a Spherical Vortex," *Phil. Trans. Roy. Soc.*, **185**, 213 (1894).

Hills, J. H., "Radial Non-Uniformity of Velocity and Voidage in a Bubble Column," *Trans. IChemE*, **52**, 1 (1974).

Joshi, J. B., and M. M. Sharma, "A Circulation Cell Model for Bubble Columns," *Trans. IChemE*, **57**, 244 (1979).

Joshi, J. B., "Axial Mixing in Multiphase Contactors—A Unified Correlation," *Trans. IChemE*, **58**, 155 (1980).

Kato, Y. M., M. Nishinaka, and S. Morooka, "Distribution of Gas Holdup in a Bubble Column," *Kagaku Kogaku Ronbunshu*, **1**, 530 (1975).

Kojima, E., H. Unno, Y. Sato, T. Chida, H. Imai, K. Endo, I. Inoue, J. Kobayashi, H. Kaji, H. Nakanishi, and K. Yamamoto, "Liquid Phase Velocity in a 5.5 m Diameter Bubble Column," *J. Chem. Eng. Japan*, **13**, 16 (1980).

Latif, B. A. J., and J. F. Richardson, "Circulation Patterns and Velocity Distributions for Particles in a Liquid Fluidised Bed," *Chem. Eng. Sci.*, **27**, 1933 (1972).

Lin, J. S., M. M. Chen, and B. T. Chao, "A Novel Radioactive Particle Tracking Facility for Measurement of Solids Motion in Gas Fluidized Beds," *AIChE J.*, **31**, 465 (1985).

Miyahara, T., S. Kaseno, and T. Takahashi, "Studies on Chains of Bubbles Rising Through Quiescent Liquid," *Can. J. Chem. Eng.*, **62**, 186 (1984).

Reese, J., R. C. Chen, J.-W. Tzeng and L.-S. Fan, "Characterization of the Macroscopic Flow Structure in Gas-Liquid and Gas-Liquid-Solid Fluidization Systems Using Particle Image Velocimetry," video presentation, *Int. Conf. on Gas-Liquid and Gas-Liquid-Solid Reactor Eng.*, Columbus, OH (Sept. 1992); *Int. Video J. Eng. Research*, in press (1993).

Rietema, K., "Science and Technology of Dispersed Two-Phase Systems—I and II: I. General Aspects," *Chem. Eng. Sci.*, **37**, 1125 (1982).

Rietema, K., and Ir. S. P. P. Ottengraf, "Laminar Liquid Circulation and Bubble Street Formation in a Gas-Liquid System," *Trans. IChemE*, **48**, T54 (1970).

Rice, R. G., and N. W. Geary, "Prediction of Liquid Circulation in Viscous Bubble Columns," *AIChE J.*, **36**, 1339 (1990).

Tang, W.-T., and L.-S. Fan, "Hydrodynamics of a Three-Phase Flu-

idized Bed Containing Low-Density Particles," *AIChE J.*, **35**, 355 (1989).
Tsuchiya, K., and O. Nakanishi, "Gas Holdup Behavior in a Tall Bubble Column with Perforated Plate Distributors," *Chem. Eng. Sci.*, **47**, 3347 (1992).
Tsuchiya, K., G.-H. Song, W.-T. Tang, and L.-S. Fan, "Particle Drift Induced by a Rising Bubble in a Liquid-Solid Fluidized Bed Containing Low-Density Particles," *AIChE J.*, **38**, 1847 (1992).
Tzeng, J.-W., "Study on Fluidized Bed Reactor—Fluid Dynamics and Bioreactor Applications," PhD Diss., The Ohio State Univ. (1991).
Ueyama, K., and T. Miyauchi, "Properties of Recirculating Turbulent Two Phase Flow in Gas Bubble Columns," *AIChE J.*, **25**, 258 (1979).
Ulbrecht, J. J., and Z. S. Baykara, "Significance of the Central Plume Velocity for the Correlation of Liquid Phase Mixing in Bubble Columns," *Chem. Eng. Commun.*, **10**, 165 (1981).
Ulbrecht, J. J., Y. Kawase, and K. F. Auyeung, "More on Mixing of Viscous Liquids in Bubble Columns," *Chem. Eng. Commun.*, **35**, 175 (1985).
Van der Akker, H. E. A., and K. Rietema, "Flow Patterns and Axial Mixing in Liquid/Liquid Spray Columns," *Trans IChemE*, **57**, 147 (1979).
Walter, J. F., and H. W. Blanch, "Liquid Circulation Patterns and Their Effect on Gas Hold-Up and Axial Mixing in Bubble Columns," *Chem. Eng. Commun.*, **19**, 243 (1983).
Whalley, P. B., and J. F. Davidson, *Inst. Chem. Engrs. Symp. Ser. on Multiphase Flow Systems*, No. 38, 55 (1974).
Whitehead, A. B., "Distributor Characteristics and Bed Properties," *Fluidization*, 2nd ed., J. F. Davidson, R. Clift, and D. Harrison, eds., Academic Press (1985).
Yang, Z., U. Rustemeyer, R. Buchholz, and U. Onken, "Profile of Liquid Flow in Bubble Columns," *Chem. Eng. Commun.*, **49**, 51 (1986).
Yoshitome, H., and T. Shirai, "The Intensity of Bulk Flow in a Bubble Bed," *J. Chem. Eng. Japan*, **3**, 29 (1970).

Manuscript received June 5, 1992, and revision received Oct. 23, 1992.